

## DIAGNOSTICS OF LASER INDUCED GRAPHITE PLASMA UNDER VARIOUS PRESSURES OF AIR, HELIUM AND ARGON

Zuhaib Haider<sup>a\*</sup>, Kashif Chaudhary<sup>a,b</sup>, Sufi Roslan<sup>b</sup>, Jalil Ali<sup>a,b</sup>, Yusof Munajat<sup>b</sup>

<sup>a</sup>Laser Center, Universti Teknologi Malaysia, 81310 UTM Johor Bahru, Johor, Malaysia

<sup>b</sup>Physics Department, Faculty of Science, Universiti Teknologi Malaysia, 81310 UTM Johor Bahru, Johor, Malaysia

### Article history

Received

15 August 2015

Received in revised form

15 November 2015

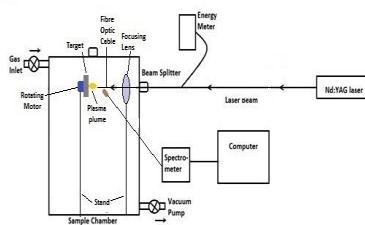
Accepted

30 December 2015

\*Corresponding author

zuhaib@utm.my

### Graphical abstract



### Abstract

Laser induced plasma provides information about the elemental composition of sample surface and through spectroscopy vital information about plasma dynamics can be obtained. In this paper we present the diagnostics of laser induced plasma at various pressures of Air, Helium and Argon gases. Graphite sample was ablated with Q-smart 850 laser while spectra were captured. Plasma parameters have been calculated by using well known methods based on Saha and Boltzmann equations. Plasma temperature was calculated relative intensity of ionic carbon lines CII 251.21 nm and CII 426.73 nm while the electron density was determined by using spectroscopic information of CI 247.85 nm and CII 426.73 nm emission lines in Saha equation. Plasma temperature and electron density were found to be dependent upon nature and pressure of the ambient atmosphere. Higher temperatures and electron densities were obtained in the presence of Air as ambient environment that is attributed to electrical and physical properties of the Air. Keeping into consideration the plasma expansion in various environments the selection of a suitable ambient pressure can be made on the basis of spectral diagnostics of plasma for a particular laser energy to obtain desirable plasma temperature and electron density suited for certain applications.

**Keywords:** Laser induced breakdown spectroscopy, graphite

### Abstrak

Aruhan plasma oleh laser memberikan maklumat mengenai komposisi elemen sesuatu sampel yang berada di permukaan dan melalui kaedah spektroskopi, maklumat penting mengenai dinamik plasma dapat diperolehi. Di dalam kertas kajian ini kami menghasilkan kaedah diagnostik pada plasma yang dihasilkan dari laser pada kepelbagaian tekanan udara, gas Helium, dan Argon. Sampel grafit dipercikkan dengan laser Q-smart 850 dimana spectrum diperolehi. Parameter plasma telah dikira dengan menggunakan kaedah bersandarkan pada persamaan Saha dan Boltzmann. Suhu plasma telah dikira relatif dengan keamatan garisan ion karbon CII 251.21 nm dan CII 426.73 nm dimana ketumpatan elektron diperolehi dengan menggunakan maklumat spektroskopi CI 247.85 nm dan CII 426.73 nm garisan pemancaran pada persamaan Saha. Suhu plasma dan ketumpatan elektron didapati bergantung pada sifat semulajadi dan tekanan sekeliling. Suhu dan ketumpatan elektron yang lebih tinggi diperolehi dalam kehadiran udara sebagai persekitaran sekeliling dimana ia disebabkan sifat fizikal dan elektrik udara. Perlu dititikberatkan perkembangan plasma dalam persekitaran yang berbeza, pemilihan tekanan sekeliling yang bersesuaian boleh dibuat pada asas diagnostik spektra plasma pada tenaga laser tertentu bagi memenuhi kehendak suhu plasma dan ketumpatan elektron yang bersesuaian untuk kegunaan tertentu.

**Kata kunci:** Aruhan laser pemecahan spektroskopi, grafit

© 2016 Penerbit UTM Press. All rights reserved

## 1.0 INTRODUCTION

Laser-induced plasma is an interesting field of study which can be utilized for various technological applications [1-4]. The study of laser induced plasma through emission spectroscopy is referred to as Laser-Induced Breakdown Spectroscopy (LIBS). LIBS can be used for qualitative and quantitative studies of materials. The first ever experimental study on laser induced plasma spectroscopy was reported in early 1960s [5].

Laser induced plasma forms when sufficiently energetic laser pulse breaks down vaporizes the material from target surface. Characteristics of laser induced plasma depends on properties of both laser and the irradiated material such as wavelength, pulse duration, irradiance for laser and aggregation state and physicochemical characteristics of the material [6, 7]. From 1980s, inexpensive options in both lasers and detectors have reached significant achievement in research field. Deposition of diamond like carbon thin films and high-temperature superconducting films are applications of laser-induced plasma. An exclusive structural and spectroscopic property of carbon molecules is an attractive point as it plays part in the various fields of study [8].

Laser induced plasma has very short temporal existence and its dynamics are totally dependent upon incident laser intensity, irradiation spot size, ambient gas composition and pressure. Electron density in the plasma can be determined with several techniques such as plasma spectroscopy, Langmuir probe, microwave and laser interferometry and Thompson scattering. Stark broadening profile can also be used to estimate the density [8-10]. A number of physical parameters contribute towards the dynamical behaviour of the plasma such as ambient environment, laser parameters, nature of material etc. The better understanding of plasma dynamics can help optimizing conditions for different applications such as growth of thin films, nano-particles etc. In this research, laser induced plasma of graphite is spectroscopically investigated. Two of the most important plasma parameters i.e., temperature and electron density are determined from the optical emission spectra obtained from laser induced plasma in ungated mode. The behaviour of carbon plasma is studied under various pressures of Air, Helium and Argon gases.

## 2.0 METHODOLOGY

Figure 1 shows the Schematic diagram of LIBS experimental setup. Experiment is performed under various pressures (300-1000 mbar) of Air, Helium and Argon gases environments. Stainless steel environment controlled sample chamber connected with

environment controlled system was utilized for this purpose. Quantel Q-smart 850 Nd:YAG laser (6 ns) operating at 740 mJ of fundamental harmonic was employed at a repetition rate of 10 Hz for sample breakdown. The laser beam entered the sample chamber through dedicated laser port fitted with quartz window and focused onto the graphite pallet by a convex lens of 18 cm of focal length. The target (graphite pallet) was continuously rotated to make fresh surface available for each incoming pulse. A 600  $\mu\text{m}$  fibre optic cable (FOC) placed inside the sealed chamber by passing through a dedicated FOC port, collected the radiations from plasma and delivered to HR4000 (Ocean Optics) spectrometer. The data was recorded without time gating using spectrasuite software. The laser energy was constantly monitored during the experiment by directing a small portion of laser energy to the energy meter. Further analyses were performed using Originlab software.

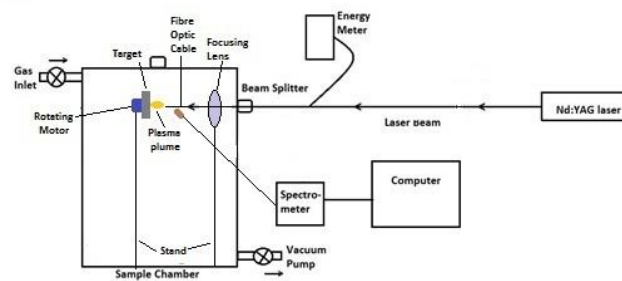
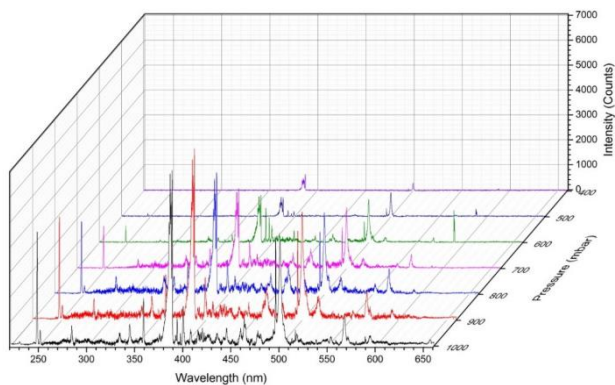


Figure 1 Schematic diagram of LIBS experimental setup

## 3.0 RESULTS AND DISCUSSION

Spectra obtained under various pressures of all three gases are presented in Figures 2-4. It is clear that the evolution of spectra is similar with increase in ambient pressure of all three gas environments. However the relative strength of spectra varies with the ambient environment. Relatively weakest spectra are obtained with Helium environment and strongest are obtained in the presence of Argon environment. It is attributed to nature of the gas. Air provides better insulation keeping the plasma hot and radiant at higher ambient pressures.

The ungated spectroscopic data recorded was subsequently utilized for plasma characterization. Two of the most important parameters of laser induced plasma i.e., temperature and density are calculated that are helpful in understanding plasma dynamics under the given circumstances. There are various methods that can serve calculation of these parameters, selection can be made depending on the method's suitability with the available data.



**Figure 2** Graphite plasma at various pressures of ambient Air

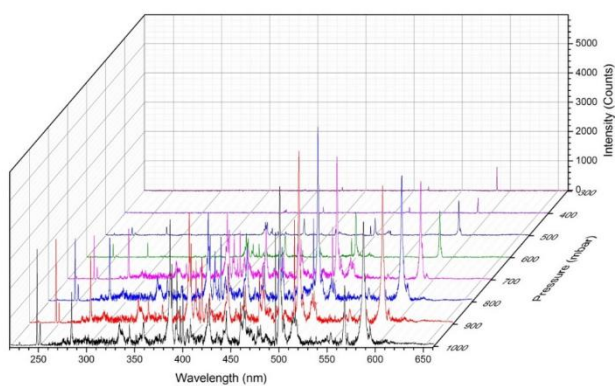


**Figure 3** Graphite plasma at various pressures of ambient Helium gas

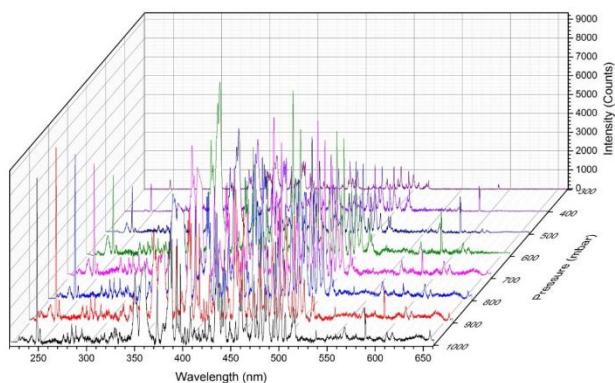


**Figure 4** Graphite plasma at various pressures of ambient Argon gas

### Plasma Temperature and Electron Density

Saha equation gives relative populations of two consecutive ionization states. Since the emission intensities are directly proportional to number of emitting species in a particular ionization state, Saha equation can be written in terms of emission line intensities as follows (Eq.1). [11]. It can be rearranged to calculate electron density in the plasma.

$$n_e = \frac{2(2\pi m_e kT)^{3/2}}{h^3} \frac{I_i \lambda_i A_i g_{i+1}}{I_{i+1} \lambda_{i+1} A_{i+1} g_i} e^{-\frac{(E_{i+1} - E_i + \chi_i)}{kT}} \quad (1)$$

where  $n_e$  ( $\text{cm}^{-3}$ ) is the electron density,  $I$  (counts) is the intensity of the spectrum,  $\lambda$  (nm) is the wavelength,  $A$  ( $\text{s}^{-1}$ ) is the transition probability,  $g$  (dimensionless) is the degeneracy,  $E$  ( $\text{cm}^{-1}$ ) is upper level energy and  $T$  (K) is the electron temperature. The constants are Planck constant,  $h$  and Boltzmann constant  $k$ . whereas, the subscript  $i$  mentions the ionization states.

The evolution of intensities shows pressure dependence. It is observed that the intensity of the spectra increases with increase in background pressure in three different environments. Argon background has the maximum intensity of emission which is approximately 9000 counts, followed by Air background which about 7000 counts, then Helium background which approximately 5000 counts. Less electron density causes less number of collisions at low background pressure resulting less emission intensity. It proves that the collision between plasma particles (electrons, ions and neutral charges) is less in low background pressure. At high background pressure, plasma emission is enhanced by the collisional excitation [12-14]. Besides, spatial confinement of plasma for a longer time and causes more radiation emission [15, 14].

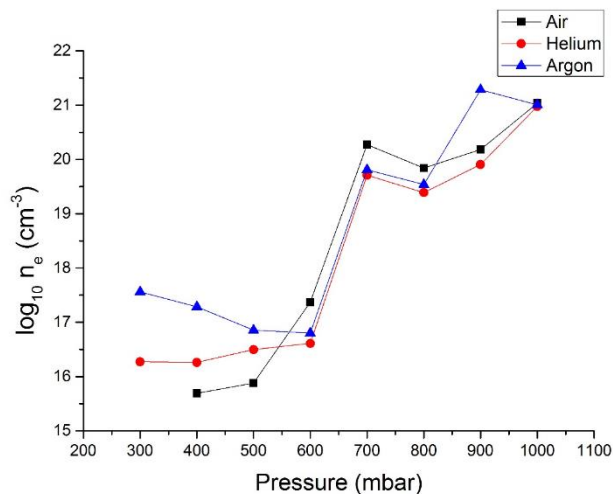


**Figure 5** Electron density in plasma for three different background gases, obtained from CII 426.73 nm and CI 247.85 nm emission lines

Tables 2 provides values of the electron density under different background (Air, Helium and Argon) at different pressures. Saha equation is used to determine the electron density using singly ionized and CII 426.73 nm line and CI 247.86 nm atomic line. The spectroscopic data used in the calculation was obtained from NIST atomic spectral database [16] as listed in Table 1.

Figure 5 illustrates the logarithm of electron density against pressure for air, Argon and Helium background. An overall increasing trend of electron

density is observed with ambient pressure of each background gas. Air background has the highest electron density followed by Argon background then Helium background. The electron density with air in the background is observed in the range of  $2.34 \times 10^{17} \text{ cm}^{-3}$  to  $1.09 \times 10^{21} \text{ cm}^{-3}$ , in helium background is in the range of  $1.82 \times 10^{16} \text{ cm}^{-3}$  to  $9.49 \times 10^{20} \text{ cm}^{-3}$  and in argon background, the electron density is in the range of  $6.34 \times 10^{17} \text{ cm}^{-3}$  to  $1.01 \times 10^{21} \text{ cm}^{-3}$ . The highest electron density achieved in this experiment with all three background gases is nearly the same, it seems to be a saturated value of electron density that can be achieved under given circumstances. However, this observation needs further verification.

**Table 1** Spectroscopic data of CI and CII lines utilized for calculating electron density and plasma temperature

Element	Wavel	Transition	Upper	Upper
	-ength	Probability	level	level
	$\lambda$ (nm)	A (s <sup>-1</sup> )	Energy	degene
			E (cm <sup>-1</sup> )	racy
CI	247.85	2.8e+07	61981.82	3
CII	251.21	5.61e+07	150461.58	6
CII	426.73	2.38e+08	168978.34	8

The increasing trend of electron density in response to the increment in ambient pressure is attributed to the fact that as the plasma plume expands in volume at low pressure which cools it down and a decrease in the electron density is observed [17]. On contrary, higher ambient pressure effectively confines and insulates plasma that results in further absorption of laser energy within the plasma and hence increment in the electron density is observed.

**Table 2** Parameters display by OSD

Pressure (mbar)	Electron Density, $n_e$ (cm <sup>-3</sup> )		
	Air	Helium	Argon
300		1.87E+16	3.63E+17
400	4.92E+15	1.82E+16	1.93E+17
500	7.57E+15	3.14E+16	7.20E+16
600	2.34E+17	4.09E+16	6.34E+16
700	1.88E+20	5.14E+19	6.47E+19
800	6.93E+19	2.45E+19	3.46E+19
900	1.52E+20	8.06E+19	1.93E+21
1000	1.09E+21	9.49E+20	1.01E+21

## Plasma Temperature

Temperature is a vital parameter in characterizing the plasma. It provides valuable information about plasma dynamics associated with ionization, dissociation and excitation of species inside the plasma. Since, plasma temperature determines population of various energy levels of species, relative intensity of emission lines belonging to same species can be used for determination of plasma temperature

assuming that the population of excited levels follow Boltzmann distribution. Intensity ratio method is therefore used to estimate the electron temperature. Boltzmann equation describes the behaviour of particles in a system based on its microscopic state. By considering two different emission lines with transitions  $i \rightarrow j$  and  $m \rightarrow n$ ; where  $i$  and  $m$  are upper energy levels,  $j$  and  $n$  are lower energy levels, the temperature can be obtained by using Eq. (3.4.2.1). These two lines are from the same ionization stage

$$T = -\frac{E_i - E_m}{k \ln \left( \frac{I_{ij} \lambda_{ij} A_{mn} g_m}{I_{mn} \lambda_{mn} A_{ij} g_i} \right)} \quad (2)$$

where  $T$  (K) is the electron temperature,  $E$  (cm<sup>-1</sup>) is upper level energy,  $I$  (counts) peak intensity of the wavelength  $\lambda$  (nm),  $A$  (s<sup>-1</sup>) is the transition probability,  $g$  is the degeneracy of upper energy level and  $k$  is the Boltzmann constant. For better accuracy of temperature measurements the difference between upper energy levels of the two emission lines should be greater than 2 eV [18].

Table 3 provides values of plasma temperature estimated at different ambient pressures of each background gas (Air, Helium and Argon). Spectral lines of singly ionized carbon i.e., CII 251.21 nm and CII 426.73 nm are used to estimate the plasma temperature at each different ambient pressure. The spectroscopic data of these emission line is obtained from NIST atomic spectra database [16] and tabulated in Table 1.

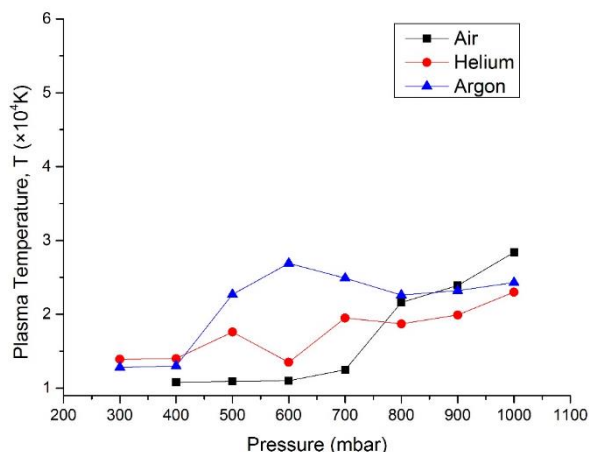


**Figure 6** Plasma temperature for three different background gases, obtained from CII 251.21 nm and CII 426.73 nm emission lines

As observed in Figure 6, plasma temperature shows an overall increasing trend with background pressure for each background gases. Argon in the ambience of plasma causes highest temperature values as compared to Air and Helium. The maximum temperatures achieved are  $6.16 \times 10^4$  K at 500 mbar,  $2.30 \times 10^4$  K at 1000 mbar and  $3.70 \times 10^4$  K at 900 mbar for air, helium and argon background respectively.

High irradiance due to high plasma temperature causes depletion of excited state due to the



excitation to higher level and de-excitation to lower level. Excitation and de-excitation causes fragmentation of excited state population. The fragments absorption heats up the plasma plume and cause increasing temperature and further fragmentation into smaller components such as atoms and ions [8]. Among those three gases, helium environment causes lowest profile compared to the other two gases. Ambient helium atmosphere cools the hot electrons down by collisions with the particles of ambient gas leading to a better thermalization thereby decreasing the temperature [8].

**Table 3** Parameters display by OSD

Pressure (mbar)	Electron Temperature, T ( $\times 10^4$ K)		
	Air	Helium	Argon
300		1.39	1.28
400	1.08	1.40	1.30
500	1.09	1.76	2.27
600	1.10	1.35	2.69
700	1.25	1.95	2.49
800	2.16	1.87	2.26
900	2.39	1.99	2.32
1000	2.84	2.30	2.43

## 4.0 CONCLUSION

Laser-induced breakdown spectroscopy (LIBS) is one of the efficient and reliable technique for the elemental analysis in a material. The electron temperature and density in different ambient background (Air, Helium and Argon) and in different pressures are crucial parameters and are determined from the laser-induced graphite plasma in this study.

Intensity ratio method is used to determine the electron temperature. The temperature is estimated by using spectral lines with same ionization states which are CII 251.21 nm and CII 426.73 nm for each different ambient pressure. The estimated electron temperature for different ambient conditions are list as follow:

- (i) The minimum electron temperature in Air is  $5.10 \times 10^4$  K at pressure of 300 mbar and the maximum is  $2.84 \times 10^4$  K at 1000 mbar.
- (ii) The minimum electron temperature in Helium is  $1.45 \times 10^4$  K at 300 mbar and the maximum is  $2.30 \times 10^4$  K at 1000 mbar.
- (iii) The minimum electron temperature in Argon is  $1.28 \times 10^4$  K at 300 mbar and the maximum is  $2.43 \times 10^4$  K at 1000 mbar.

Electron density is determined by using spectroscopic details of singly ionized CII 426.73 nm line and neutral CI 247.70 nm line in Saha equation. Estimated values for electron density are given as follow:

- (i) The minimum electron density in Air is  $3.98 \times 10^{17}$  cm<sup>-3</sup> at pressure of 300 mbar.

Meanwhile, the maximum is  $1.09 \times 10^{21}$  cm<sup>-3</sup> at 1000 mbar.

- (ii) The minimum electron density in Helium is  $4.81 \times 10^{16}$  cm<sup>-3</sup> at pressure of 300 mbar. Meanwhile, the maximum is  $9.49 \times 10^{20}$  cm<sup>-3</sup> at 1000 mbar.
- (iii) The minimum electron density in Argon is  $3.88 \times 10^{17}$  cm<sup>-3</sup> at pressure of 300 mbar. Meanwhile, the maximum is  $1.01 \times 10^{21}$  cm<sup>-3</sup> at 1000 mbar.

Observation of emission spectrum demonstrates that emission intensities increase with increase in the background pressure. Besides, from the obtained results, both electron density and plasma temperature have increasing trend with ambient pressure. Both electron density and plasma temperature are highest with Air background as compared to the other gases. In conclusion, the spectroscopic investigations of the graphite plasma show dependence of ambient environment on plasma dynamics.

## Acknowledgement

We would like to thank Laser Center, ISI-SIR, Universiti Teknologi Malaysia and MyBrain15 under Ministry of Education (MoE) and for financial support. This study is supported by GUP grant.

## References

- [1] Ferreira, E. C., Gomes Neto, J. A., Milori, D. M. B. P, Ferreira, E. J. and Anzano J. M. 2015. Laser-Induced Breakdown Spectroscopy: Extending Its Application To Soil pH Measurements. *Spectrochimica Acta Part B: Atomic Spectroscopy*. 110: 96-99.
- [2] Gasda, P. J., Acosta-Maeda, T. E., Lucey, P. G., Misra, A. K., Sharma S. K. and Taylor G. J. 2015. Next Generation Laser-Based Standoff Spectroscopy Techniques for Mars Exploration. *Applied Spectroscopy*. 69(2): 173-192.
- [3] Guirado, S., Fortes, F. J. and J. J. Laserna. 2015. Elemental Analysis Of Materials In An Underwater Archeological Shipwreck Using A Novel Remote Laser-Induced Breakdown Spectroscopy System. *Talanta*. 137: 182-188.
- [4] Iqbal, J., Mahmood, S., Tufail, I., Asghar, H., Ahmed, R. and Baig, M. A. 2015. On The Use Of Laser Induced Breakdown Spectroscopy To Characterize The Naturally Existing Crystal In Pakistan And Its Optical Emission Spectrum. *Spectrochimica Acta Part B: Atomic Spectroscopy*. 111: 80-86.
- [5] Radziemski, L. J. 2002. From LASER to LIBS, The Path Of Technology Development. *Spectrochimica Acta Part B: Atomic Spectroscopy*. 57: 1109-1113.
- [6] Gaudio, R., Dell'Aglio, M., Pascale, O. D., Senesi, G. S. and Giacomo, A. D. 2010. Laser Induced Breakdown Spectroscopy For Elemental Analysis In Environmental, Cultural Heritage And Space Applications: A Review Of Methods And Results. *Sensors*. 10(8): 7434-7468.
- [7] Cremers, D. A. and Radziemski, L. J. 2013. *Handbook of Laser-Induced Breakdown Spectroscopy*. Wiley.
- [8] Harilal, S., Issac, R. C., Bindhu, C., Nampoory, V. and Vallabhan, C. 1997. Optical Emission Studies Of Species In Laser-Produced Plasma From Carbon. *Journal of Physics D: Applied Physics*. 30(12): 1703-1709.

- [9] Hegazy, H., Abdel-Wahab, E. A., Abdel-Rahim, F. M., Allam, S. H. and Nossair, A. M. A. 2013. Laser-Induced Breakdown Spectroscopy: Technique, New Features, And Detection Limits Of Trace Elements In Al Base Alloy. *Applied Physics B*. 115(2): 173-183.
- [10] Cirisan, M., Cvejić, M., Gavrilović, M., Jovičević, S., Konjević, N., and Hermann, J. 2014. Stark Broadening Measurement Of Al II Lines In A Laser-Induced Plasma. *Journal of Quantitative Spectroscopy And Radiative Transfer*. 133: 652-662.
- [11] Canal, G., Luna, H., Galvao, R. and Castell, R. 2009. An Approach To A Non-LTE Saha Equation Based On The Druyvesteyn Energy Distribution Function: A Comparison Between The Electron Temperature Obtained From OES And The Langmuir Probe Analysis. *Journal of Physics D: Applied Physics*. 42(13): 135202-135207.
- [12] Yalçın, S., Tsui, Y. Y. and Fedosejevs, R. 2004. Pressure Dependence Of Emission Intensity In Femtosecond Laser-Induced Breakdown Spectroscopy. *Journal of Analytical Atomic Spectrometry*. 19(10): 1295-1301.
- [13] Singh, J. P. and Thakur, S. N. 2007. *Laser-Induced Breakdown Spectroscopy*. Elsevier Science.
- [14] Haider, Z., Ali, J., Arab, M., Munajat, Y. b., Roslan, S., Kamarulzman, R. Bidin, N. 2015. Plasma Diagnostics And Determination Of Lead In Soil And Phaleria Macrocarpa Leaves By Ungated Laser Induced Breakdown Spectroscopy. *Analytical Letters* (Accepted for publication).
- [15] Chaudhary, K., Rosalan, S., Aziz, M., Bohadoran, M., Ali, J., Yupapin, P. and Bidin, N. 2015. Laser-Induced Graphite Plasma Kinetic Spectroscopy under Different Ambient Pressures. *Chinese Physics Letters*. 32(4): 043201.
- [16] Data retrieved from <http://physics.nist.gov/cgi-bin/ASD/lines1.pl>.
- [17] Ruiz, M., Guzmán, F., Favre, M., Hevia, S., Correa, N., Bhuyan, H., Wynham, E. and Chuaqui, H. 2014. Characterization Of A Laser Plasma Produced From A Graphite Target. *Journal Of Physics: Conference Series*. IOP Publishing.
- [18] Hegazy, H., El-Ghany, H. A., Allam, S. and El-Sherbini, T. M. 2013. Spectral Evolution Of Nano-Second Laser Interaction With Ti Target In Air. *Applied Physics B*. 110: 509-518.
- [19]